Ab Initio Investigation of the Structural and Electronic Properties of the Molecules and Crystals of Tetraphenyl Derivatives of Group IVA Elements

Tingting Lin, Xue-Ming Liu, and Chaobin He*

Institute of Materials Research & Engineering (IMRE), 3 Research Link, Singapore 117602

Received: June 27, 2004; In Final Form: August 25, 2004

The structural and electronic properties of molecular and crystalline $X(C_6H_5)_4$ (X = C, Si, Ge, Sn, Pb) have been studied systematically by ab initio/DFT calculations at the level of GGA-PW91 with either a plane wave basis set and ultrasoft pseudopotentials or with a local basis set−double numerical plus polarization (DNP) and all electrons. The optimized geometrical parameters were found to be comparable to the results of X-ray crystallographic, gas-phase electron diffraction, and two reported calculations for CPh_4 and $SiPh_4$ molecules. In addition, the electronic and optical properties such as band structures, molecular orbitals, the energy gap between the lowest unoccupied orbital (LUMO) and the highest occupied orbital (HOMO), density of states (DOS), partial density of states (PDOS), refractive indices and absorption spectra etc can be obtained from the calculations at the optimized structures. The calculated LUMO−HOMO gap is 4.1−4.6 eV. The simulated absorption spectra of XPh_4 are similar. The effect of the central atom on the HOMO, the LUMO, and other frontier molecular orbitals is increased as the atomic number of the central atom increases. Our studies showed that the present computational methods were good approximations and cost-effective for the medium-sized molecules and could be extended to the large-sized tetrahedral chromophore molecules.

Introduction

Creating tetrahedral-shaped molecules is one of the important strategies to prevent small conjugated organic molecules from crystallization spontaneously and render them amorphous in nature, which are critical for optoelectronic applications. Recently, various derivatives of tetraphenylmethane and tetraphenylsilane have been designed, synthesized and investigated.[1−16] It has been proven experimentally that attaching four identical chromophores to a central carbon atom tetrahedrally causes only a modest perturbation to the resulting electronic characteristics of chromophoric arms.[6] The crystal structures of the tetraphenyl derivatives of the main group IV elements (XPh_4: X = C, Si, Ge, Sn, Pb) have been determined and re-determined by single-crystal X-ray crystallography.[17−32] It was found that these compounds crystallize in the tetragonal system. The space group is $P42_1c$ (international table number 114), which has eight equivalent positions. Because every unit cell contains two molecules, the central atoms of the molecules must occupy special positions: (0 0 0) and ($^1/_2a$ $^1/_2b$ $^1/_2c$), whereas the atoms of the phenyl groups are in general positions with the restriction that the molecule has a $\bar{4}$(S_4) symmetry. Gas-phase molecular structures of tetraphenylsilane, tetraphenylgermane, and tetraphenyltin were also determined by electron diffraction.[33]

Compared to the extensive experimental investigations, theoretical studies on the molecular and crystalline structures of XPh_4 remain rare. Ahmed et al. used atom−atom potentials to determine the conformation of the molecules of XPh_4 (X = C, Si, Sn, Pb) in the gaseous phase and in the crystalline state.[34] The potential curve becomes flatter with the increase in the C−X bond length of Ph−C and the central atom (X). In other words, the possible range of rotation of the phenyl groups increases as their distance to the central atom increases (C−C = 1.50, Si−C = 1.84, Sn−C = 2.14, and Pb−C = 2.29 Å). The crystal structure of the molecule may be influenced by intermolecular interactions, in addition to intramolecular interactions. Mislow and co-workers carried out stereochemical analysis;[35,36] empirical force field[37,38] and its hybrid with extended Hückel molecular orbital[39] calculations for the free molecules of tetraarylmethanes and tetraarylsilanes. The superimposition of four 2-fold rotors (in this case, phenyl groups) onto a skeleton of T_d symmetry brings about the removal of all four 3-fold symmetry axes and the Ar_4X system can therefore never adopt T_d symmetry, but must belong to one of the seven subgroups of D_{2d} (D_{2d}, D_2, S_4, C_{2v}, C_2, C_s, C_1). Semiempirical calculations and NMR spectroscopic studies were carried out for $Ph_{4-n}X(p\text{-Tol})_n$ ($n = 0-4$, X = Si, Ge, Sn, Pb) by Charissé et al.[40] They found that a change of the symmetry of the formally tetrahedral XC_4 backbone arises if X = Si and Ge (elongation along one S_4 or C_3 axis) are altered to X = Sn and Pb (contraction along S_4 axis). Recently, as the computer capacity increases, accurate ab initio computations are affordable for these medium-sized molecules. Ab initio/DFT calculations at the HF/6-31(d,p) and B3LYP/6-31G(d,p) levels have been done for tetraphenylmethane and tetraphenylsilane molecules by Knop et al.[41] and Campanelli et al.,[42] respectively. Their studies confirmed that the ground-state conformations of the two free molecules have a S_4 symmetry.

Most of the previous theoretical studies were focused on the molecular conformations and geometries. No ab initio calculations have been found for the five XPh_4 crystals and the other three isolated XPh_4 (X = Ge, Sn, Pb) molecules. In this work, we shall present the ab initio/DFT calculation results for all five compounds in both molecular and crystalline states. An ab initio total energy program (CASTEP[43] with plane waves basis and core treatment: ultrosoft pseudopotentials) and a density functional theory electronic structure program (DMol^3 [44,45] with double numerical plus polarization (DNP) basis and no special treatment for atomic cores (i.e., all electrons are included in the calculations)) were employed to fully optimize single molecules and crystals of the tetraphenyl family XPh_4 (X = C, Si, Ge, Sn, Pb). The optimized structural parameters were compared

* To whom correspondence should be addressed. E-mail address: cbhe@imre.a-star.edu.sg.

10.1021/jp047214d CCC: $27.50
Published on Web 10/16/2004

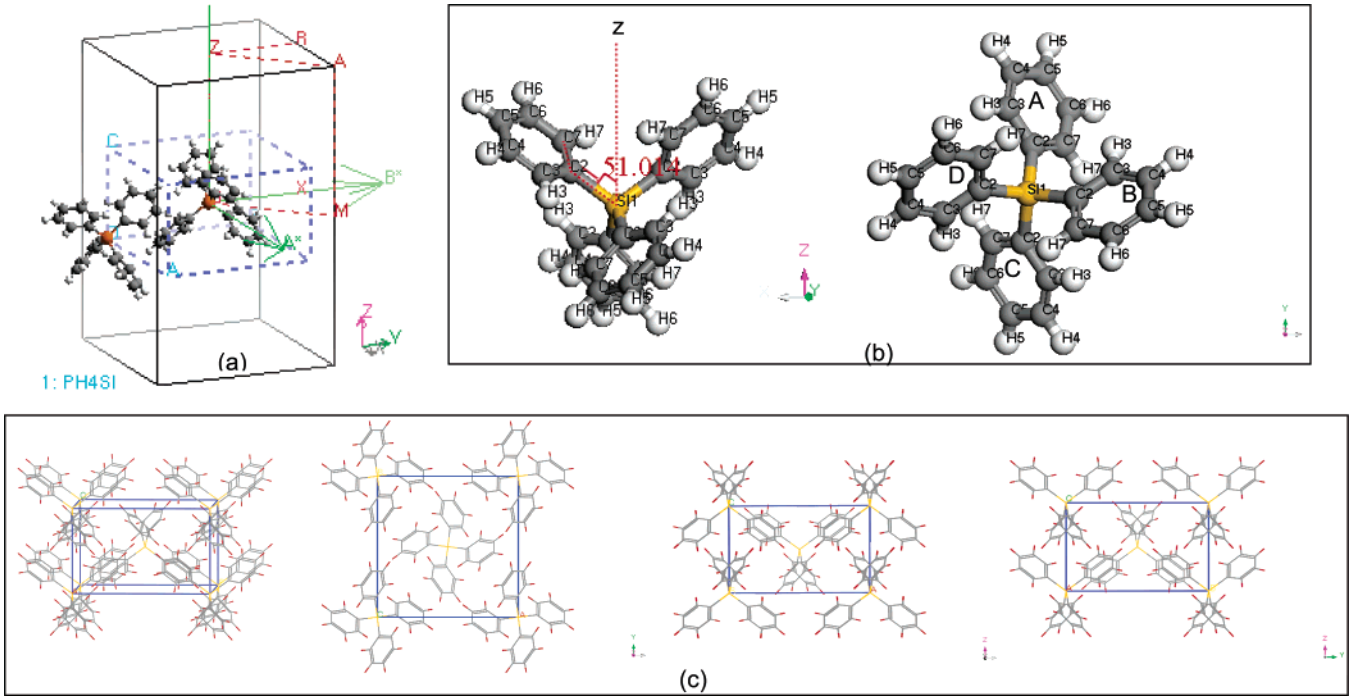

Figure 1. (a) $SiPh_4$ crystal. Key: unit cell, blue; Brillouin zone, black; high symmetry point, red characters; path, red; reciprocal axes, light green. (b) Definition of the torsion angle C7−C2−Si−Z: the angle between the plane determined by the S_4 axis (or *z*-axis) and bond C−X and the phenyl plane, the atomic numbering. (c) Molecular packing in the crystals XPh_4. 3D, on *XY*, *XZ*, and *YZ* planes.

to the X-ray crystallographic, the electron diffraction, and the theoretical calculation results reported in the literature.[17−19,22−33,41,42] Band structures, band gaps, and refractive indices (for crystals); the HOMO, LUMO, and the LUMO−HOMO gap or other molecular orbital (MO) energies, shapes (for molecules); DOS, PDOS, optical absorption spectra, etc., important electronic and optical properties, in addition to the geometrical parameters, can be derived from the optimized structures. Therefore it provides a useful and consistent method to investigate the relation between structures and properties. Although the XPh_4 are the smallest structures of tetrahedral chromophores, high-level computations are very CPU time and main memory demanding. The approaches we used are reasonable approximations and can be applied to study larger and more complicated XPh_4 based light emitting molecules. Moreover, a comparison of crystals and single molecules results will illustrate the molecules interaction and packing effect on the optical properties and the crystal field effect on molecular electronic structure. A comparative study of the five molecules together will reveal the perturbation of the phenyl ring by the central atoms and the contribution of the central atoms to the frontier molecular orbitals.

TABLE 1: Structure of XPh_4 Molecular Crystals (Standard Deviations in Parentheses)

compound	CCDC refcode	X−C (Å)	*a* (Å)	*c* (Å)	remarks
$C(C_6H_5)_4$	TEPHME	1.47	10.87	7.23	ref 17
$C(C_6H_5)_4$	TEPHME02	1.551(3)	10.894(2)	7.280(1)	ref 18
	TEPHME03	1.550(3)	10.899(2)	7.279(1)	
	TEPHME11	1.550(3)	10.916(3)	7.287(2)	
$C(C_6H_5)_4$	PH4C00	1.549(2)	10.9050(10)	7.2850(5)	ref 19[a]
$C(C_6H_5)_4$		1.53(4)	11.037(7)	7.415(6)	this work[b]
$Si(C_6H_5)_4$	TPENSI	1.872(7)	11.46(1)	7.09(3)	ref 22
$Si(C_6H_5)_4$	TPENSI03	1.877(2)	11.450(2)	7.063(1)	ref 23
$Si(C_6H_5)_4$	PH4SI0	1.8730(19)	11.4476(9)	7.0644(6)	ref 19[a]
$Si(C_6H_5)_4$		1.86(7)	11.562(4)	7.195(7)	this work[b]
$Ge(C_6H_5)_4$	TPENGE	1.956(1)	11.613(4)	6.904(2)	ref 24
	TPENGE01	1.952(1)			
$Ge(C_6H_5)_4$	TPENGE02	1.957(4)	11.656(11)	6.928(7)	ref 25
$Ge(C_6H_5)_4$	PH4GE0	1.952(3)	11.6160(5)	6.9020(3)	ref 19[a]
$Ge(C_6H_5)_4$		1.92(3)	11.747(9)	7.022(9)	this work[b]
$Sn(C_6H_5)_4$	TPHESN	2.144(14)	12.058(1)	6.568(1)	ref 26
$Sn(C_6H_5)_4$	TPHESN01	2.143(10)	11.97(3)	6.60(2)	ref 27
$Sn(C_6H_5)_4$	TPHESN02	2.139(4)	12.058(1)	6.58(1)	ref 28
$Sn(C_6H_5)_4$	TPHESN03	2.143(5)	12.068(3)	6.558(2)	ref 29
$Sn(C_6H_5)_4$	PH4SN0	2.143(3)	12.0680(4)	6.5570(3)	ref 19[a]
$Sn(C_6H_5)_4$		2.13(0)	12.218(9)	6.686(9)	this work[b]
$Pb(C_6H_5)_4$	TPHEPB	2.19(3)	12.092(3)	6.589(2)	ref 30
$Pb(C_6H_5)_4$	TPHEPB01	2.194(6)	12.151(2)	6.545(1)	ref 31
$Pb(C_6H_5)_4$	TPHEPB02	2.202(9)	12.144(1)	6.547(1)	ref 32
$Pb(C_6H_5)_4$	PH4PB0	2.227(9)	12.1110(9)	6.5430(4)	ref 19[a]
$Pb(C_6H_5)_4$		2.24(9)	12.253(6)	6.673(2)	this work[b]

[a] See ref 19 footnote: full crystallographic data for Ph_4X (X = Pb, Sn, Ge, Si, C). CCDC reference numbers 185087−185091. [b] This work, CASTEP geometry optimization, gga-pw91, ultrasoft pseudopotential, plane wave cutoff 280 eV (fine).

Computational Methods

Quantum mechanics provides a reliable way to calculate the structural and electronic properties of materials because it deals with both nuclei and electrons and their interactions simultaneously. The many-body problem is the challenge. With the development of theories, approximation methods, fast algorithms, and computer power (speed, memory, parallel machines), the first principles computations become feasible for medium and large scale systems. Software modules CASTEP and DMol[3] within the Materials Studio v3.0 package (Accelrys Inc. 2003) have been employed to fully optimize isolated molecules and crystals of XPh_4 (X = C, Si, Ge, Sn, Pb). All the calculations were done on a SGI Altrix3000 parallel server. The nonlocal gradient-corrected exchange-correlation functional in the form parametrized by Perdew and Wang (GGA-PW91)[46] was used. For the calculation of molecular crystals of XPh_4, we used *k* points in the irreducible Brillouin zone determined according to the Monkhorst and Pack scheme.[47] A finite basis correction[48,49] was considered to confirm the convergence of the calculations. Structural optimizations were performed by using

TABLE 2: Total Energies

compound	crystal[a] (2 molecules/cell) CASTEP total energy (eV)	single molecule[b] CASTEP total energy (eV)	single molecule[c] DMol^3 total energy (ha)	cohesive energy[d] (kcal/mol)	latent heat of sublimation (at 25 °C)[e] (kcal/mol)
CPh_4	−8441.6293113	−4220.2697384	−964.6561484	12.57	
	(−8411.2179043)	(−4220.1802239)	(−964.0560354)		
$SiPh_4$	−8348.7406570	−4173.5767777	−1216.0873246	18.30	12.18
	(−8332.454925)	(−4173.5051728)	(−1215.7535953)		
$GePh_4$	−8348.2586625	−4173.4802340	−3003.7824740	14.97	13(estd)
	(−8319.123764)	(−4173.3542138)	(−3003.203049)		
$SnPh_4$	−8323.3201831	−4160.9584797	−6952.3613932	16.18	14.21
	(−8304.8061852)	(−4160.900795)	(−6951.9831184)		
$PbPh_4$	−11453.0636750	−5725.7651928	−20456.0595272	17.68	19.8
	(−11429.8492728)	(−5725.7290426)	(−20455.581397)		

[a] This work, CASTEP, crystal, geometry optimization, gga-pw91, ultrasoft pseudopotential, plane wave cutoff 280 eV. Values in brackets are single point energy calculation results at the experimental lattice constants and molecules geometries. [b] This work, CASTEP, single molecule, geometry optimization, gga-pw91, ultrasoft pseudopotential, plane wave cutoff 280 eV supercell (cubic) size: 20 Å, the values in brackets are the geometry oprtimization results when cell size is 16 A. [c] This work, DMol^3, single molecule, geometry optimization, gga-pw91, all electrons, DNP cutoff 5.5 Å. Values in brackets are single point energy calculation results at molecular geometries in the experimental crytsal. [d] Cohesive energy (per molecule) = $(2E_T(\text{molecular } XPh_4) - E_T(\text{crystalline } XPh_4))/2$ from CASTEP calculations. [e] Newkirk, H. W. *J. Organomet. Chem.* **1972**, *44*, 263.

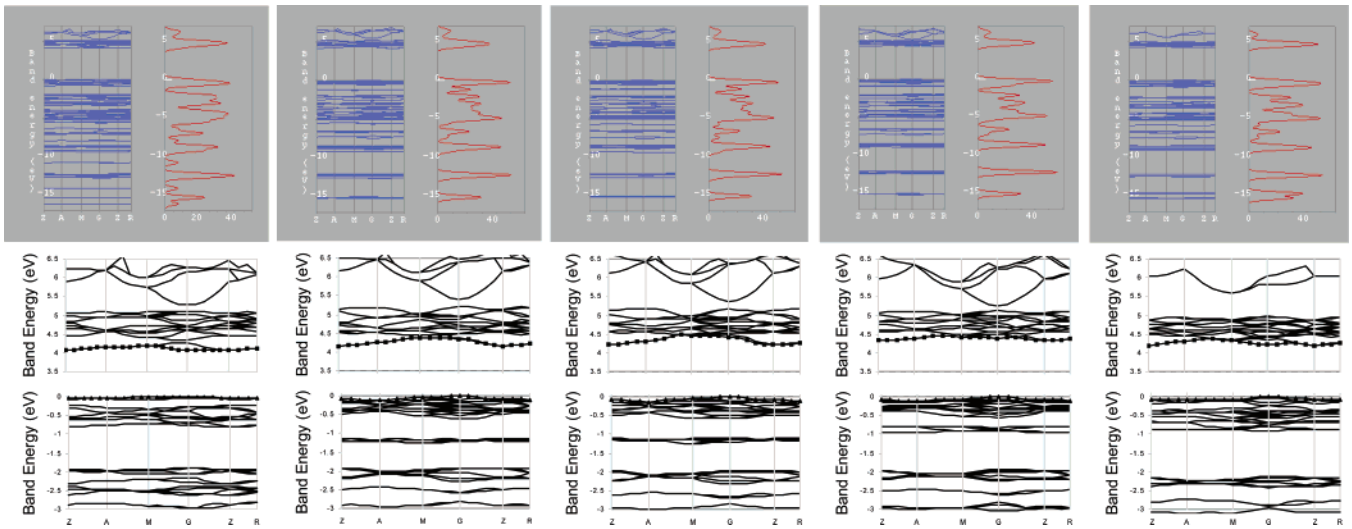

Figure 2. CASTEP band structure for XPh_4 (X = C, Si, Ge, Sn, Pb) crystals: geometry optimization; band energy range −17 to +7 eV; DOS 0−50 (CPh_4) and 0−60 (others) electrons/eV; valence bands −3 to 0 eV; conduction bands 3.5−6.5 eV.

the BFGS minimization technique.[50] Molecular calculations were performed using the supercell approach (CASTEP). Details of the general methods have been provided in an earlier paper.[51] Optimizations with supercell sizes of 16 and 20 Å have been carried out and compared to make sure the convergence related to the cell size. All electron calculations for the molecules were done using DMol^3 with double numerical plus polarization (DNP) local basis (a cutoff radius of 5.5 Å). The DNP basis is comparable to Gaussian 6-31G(d,p) sets. For examples: H, 1s 1s′ 1p; C, 1s 2s 2p 2s′ 2p′ 3d; Si, 1s 2s 2p 3s 3p 3s′ 3p′ 3d. In DMol^3 basis functions are given numerically as values on an atomic-centered spherical-polar mesh, rather than as analytical functions (i.e., Gaussian orbitals). The angular portion of each function is the appropriate spherical harmonic $Y_{lm}(\theta,\varphi)$. The radial portion is obtained by solving the atomic DFT equations numerically. Hence it is faster and can be applied to larger molecules.

Results and Discussions

Total Energy and Structural Feature. The solid XPh_4 (X = C, Si, Ge, Sn, Pb) have been well-refined crystallographically.[17−32] The initial unit cells are obtained from Cambridge crystallographic data center (CCDC) and ref 19. All the five crystals have similar structures. A typical unit cell is shown in Figure 1a for crystalline tetraphenylsilane as an example. There are two molecules in the unit cell and the space group is $P\bar{4}2_1c$. The corresponding Brillouin zone (BZ) together with symmetry directions is also shown. Full structure optimizations of both lattice parameters and atomic positions were performed. For a comparison, single point energy calculations were carried out as well at the initial experimental lattice constants and molecular geometries.[19] The optimized lattice constants and the bond lengths of X−C are summarized in Table 1 with corresponding results of some X-ray diffraction (XRD) results available in references. The calculated bond lengths of X−C are in good agreement with the experimental results whereas the optimized lattice constants are slightly larger (∼0.1 Å) than the related XRD lattice constants. The discrepancies were probably caused by the differences of temperatures (X-ray diffraction experiments are usually carried out at room temperature). The total energies obtained are listed in the first column of Table 2. For a comparison, the total energies at the initial structures of the crystals are included in the brackets too.

Optimizations for isolated molecules were performed using two methods: CATSEP supercell method and DMol^3 molecule.

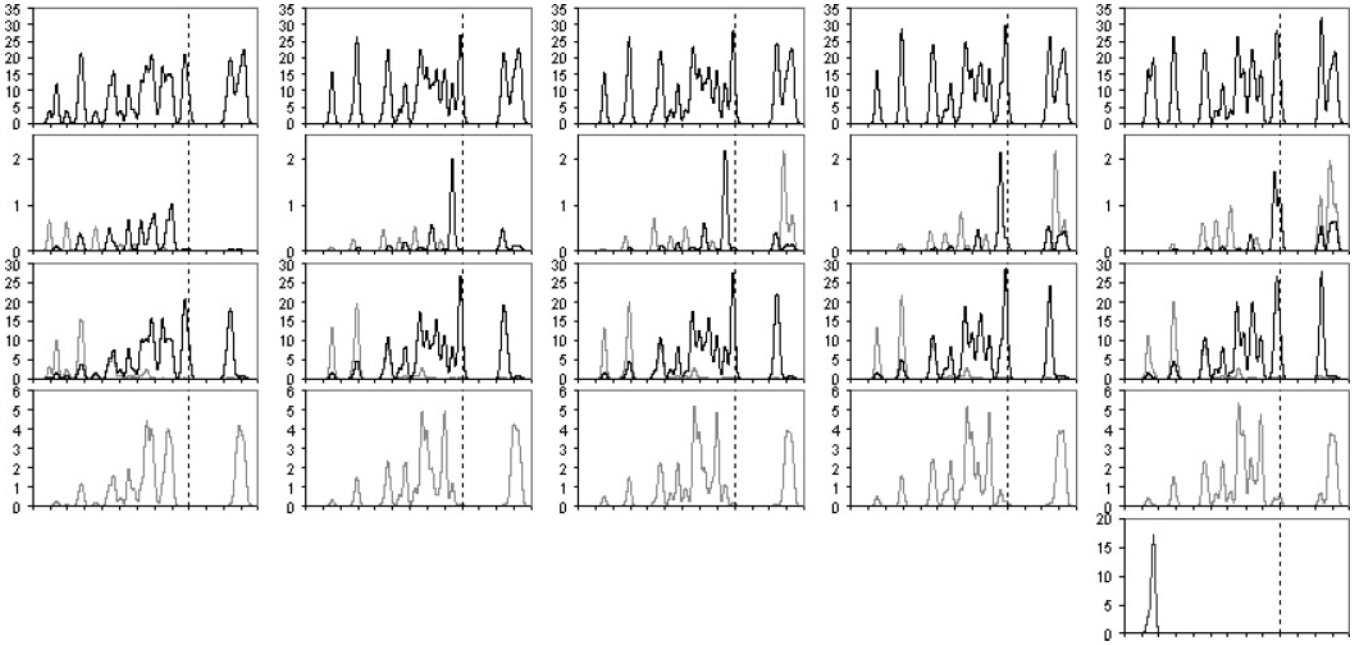

Figure 3. CASTEP DOS and PDOS for isolated XPh_4 molecules, 20 empty orbitals have been added. From left to right columns are for XPh_4, X = C, Si, Ge, Sn, Pb, respectively. First row: total density of states (DOS). Second row: partial density of states (PDOS) for the central atoms C, Si, Ge, Sn, and Pb. Light curves are for the −s component and dark curves for the −p component. Third row: PDOS for all C atoms on the four phenyl rings. Fourth row: PDOS for all H atoms on the phenyls. The panel in the last row and column is the PDOS for the central atom Pb of $PbPh_4$, −d component. *X* axes are band energies, each unit represents 2 eV, range −18 to +8 eV. *Y* axes are either DOS or PDOS, in electrons/eV. Dotted lines indicated the Fermi energy (0 eV) positions.

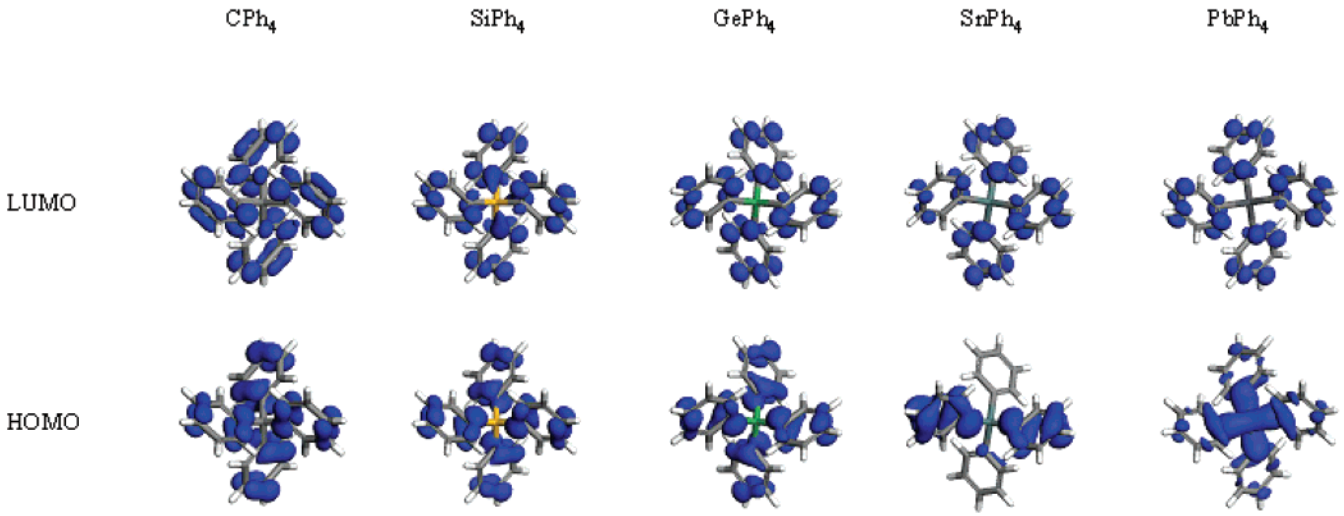

Figure 4. HOMOs and LUMOs of XPh_4 (X = C, Si, Ge, Sn, Pb) molecules, isovalue = 0.01.

The calculated total energies are shown in the second and third columns of Table 2, respectively. The CASTEP supercell calculations were performed twice for each molecule XPh_4 with different supercell sizes: 16 and 20 Å. The small discrepancies shown in the total energies for the same molecule confirmed the convergences related to the box sizes.

The optimized molecular geometrical parameters in both solid and gaseous phases are listed in Table 3 with the previous experimental results and DFT calculation results reported in the literature for CPh_4 and $SiPh_4$. The other three compounds' geometrical parameters are not given here but are provided in the Supporting Information for simplicity. The atomic numberings and the definition of the torsion angle of phenyl ring are shown in Figure 1b. Overall, the optimized geometries of the molecules agree well with the existing experimental results and ab initio/DFT calculation results (using Gaussian basis sets). The molecules have a conformation of S_4 symmetry. Our calculated bond lengths of C−H on the phenyl rings are generally about 0.1 Å longer than the crystallographic results (which are usually estimations). Our DFT calculation results provided the concrete quantitative evidences for the qualitative analysis results obtained by Charissé et al.[40] That is, the C_{2v} local symmetry of the phenyl groups lowers the symmetry at the central atoms from T_d to S_4, which causes the six tetrahedral C−X-C angles to split into two groups. Though the tetrahedron in compounds with a bond length X−C smaller than 2.0 Å (X = C, Si, Ge) is always elongated (two angles less and four angles greater than the tetrahedral value 109.5°), the tetrahedron in compounds with d(X−C) > 2.0 Å (X = Sn, Pb) is always contracted (two angles greater and four angles less than the tetrahedral value) along its S_4 axis. In all cases, the average of the six angles C−X−C is close to the ideal tetrahedral value 109.5°. As the bond length of X−C increases (X = C, Si, Ge, Sn, Pb), the deviations of angles of C−C−C on the phenyl rings

TABLE 3: Geometrical Parameters (Bond Lengths in Angstroms; Angles in Degrees)

1. Geometrical Parameters (CPh_4)

	crystal		single molecule			
	X-ray diffraction[a]	CASTEP gga-pw91 ultrasoft PP PW 280 eV[b]	CASTEP gga-pw91 ultrasoft PP PW 280 eV cell 16 A[c]	CASTEP gga-pw91 ultrasoft PP PW 280 eV cell 20 A[c]	DMol^3 gga-pw91 all electrons DNP 5.5 A[d]	Gaussian98 B3LYP6-31G(d,p)[e]
X_1-C_2	**1.549**	**1.534**	**1.536**	**1.536**	**1.553**	**1.554**
$(C-C)_{mean}$	**1.381**	**1.384**	**1.383**	**1.383**	**1.399**	**1.388**
$(C-H)_{mean}$	**0.915**	**1.083**	**1.084**	**1.084**	**1.090**	**1.075**
$C_{2A}-X_1-C_{2B}$	110.9	110.9	111.1	111.0	111.0	112.1
$C_{2B}-X_1-C_{2C}$	110.9	110.9	111.1	111.0	111.0	112.1
$C_{2C}-X_1-C_{2D}$	110.9	110.9	111.1	111.0	111.0	112.1
$C_{2D}-X_1-C_{2A}$	110.9	110.9	111.1	111.0	111.0	112.1
$C_{2B}-X_1-C_{2D}$	106.7	106.7	106.2	106.5	106.5	104.3
$C_{2A}-X_1-C_{2C}$	106.7	106.7	106.2	106.5	106.5	104.3
$(C-X-C)_{mean}$	109.5	109.5	109.5	109.5	109.5	109.5
$C_2-C_3-C_4$	121.5	121.1	121.2	121.1	121.1	121.9
$C_3-C_4-C_5$	120.5	120.4	120.5	120.6	120.5	120.3
$C_4-C_5-C_6$	119.4	119.1	119.0	119.0	119.0	118.9
$C_5-C_6-C_7$	119.9	120.6	120.3	120.4	120.3	120.6
$C_6-C_7-C_2$	121.8	121.1	121.3	121.3	121.4	121.6
$C_7-C_2-C_3$	**116.8**	**117.9**	**117.7**	**117.6**	**117.7**	**116.7**
$(C-C-C)_{mean}$	120.0	120.0	120.0	120.0	120.0	120.0
deviation of $C_2-C_3-C_4$	−1.5	−1.1	−1.2	−1.1	−1.1	−1.9
deviation of $C_3-C_4-C_5$	−0.5	−0.4	−0.5	−0.6	−0.5	−0.3
deviation of $C_4-C_5-C_6$	0.6	0.9	1.0	1.0	1.0	1.1
deviation of $C_5-C_6-C_7$	0.1	−0.6	−0.3	−0.4	−0.3	−0.6
deviation of $C_6-C_7-C_2$	−1.8	−1.1	−1.3	−1.3	−1.4	−1.6
deviation of $C_7-C_2-C_3$	3.2	2.1	2.3	2.4	2.3	3.3
torsion angle C_7-C_2-X-Z[h]	**48.3**	**48.6**	**49.1**	**49.1**	**47.8**	

2. Geometrical Parameters ($SiPh_4$)

	crystal		single molecule				
	X-ray diffraction[a]	CASTEP gga-pw91 ultrosoft PP PW 280 eV[b]	CASTEP gga-pw91 ultrosoft PP PW 280 eV cell 16 A[c]	CASTEP gga-pw91 ultrasoft PP PW 280 eV cell 20 A[c]	DMol^3 gga-pw91 all electrons DNP 5.5 A[d]	Gaussian98 B3LYP/6-31G(d)[f]	electron diffraction[g]
X_1-C_2	**1.873**	**1.867**	**1.850**	**1.874**	**1.893**	**1.894**	**1.871**
$(C-C)_{mean}$	**1.378**	**1.387**	**1.385**	**1.389**	**1.401**	**1.400**	**1.403(3)**
$(C-H)_{mean}$	**0.958**	**1.084**	**1.085**	**1.085**	**1.091**	**1.087**	**1.087(4)**
C_{2A}-X_1-C_{2B}	110.2	109.7	110.2	110.4	110.2	109.9	
$C_{2B}-X_1-C_{2C}$	110.2	109.7	110.2	110.4	110.2	109.9	
$C_{2C}-X_1-C_{2D}$	110.2	109.7	110.2	110.4	110.2	109.9	
$C_{2D}-X_1-C_{2A}$	110.2	109.7	110.2	110.4	110.2	109.9	
$C_{2B}-X_1-C_{2D}$	108.0	109.1	108.0	107.6	108.0	108.6	
$C_{2A}-X_1-C_{2C}$	108.0	109.1	108.0	107.6	108.0	108.6	
$(C-X-C)_{mean}$	109.5	109.5	109.5	109.5	109.5	109.5	
$C_2-C_3-C_4$	121.4	121.4	121.2	121.5	121.1	121.3	
$C_3-C_4-C_5$	120.7	120.0	119.9	120.2	120.1	120.1	
$C_4-C_5-C_6$	119.6	119.7	119.8	119.4	119.7	119.7	
$C_5-C_6-C_7$	120.0	120.0	119.9	120.1	120.0	120.0	
$C_6-C_7-C_2$	121.6	121.4	121.3	121.6	121.2	121.4	
$C_7-C_2-C_3$	**116.6**	**117.5**	**117.9**	**117.2**	**117.8**	**117.5**	**118.2(4)**
$(C-C-C)_{mean}$	120.0	120.0	120.0	120.0	120.0	120.0	
deviation of $C_2-C_3-C_4$	−1.4	−1.4	−1.2	−1.5	−1.1	−1.3	
deviation of $C_3-C_4-C_5$	−0.7	0.0	0.1	−0.2	−0.1	−0.1	
deviation of $C_4-C_5-C_6$	0.4	0.3	0.2	0.6	0.3	0.3	
deviation of $C_5-C_6-C_7$	0.0	0.0	0.1	−0.1	0.0	0.0	
deviation of $C_6-C_7-C_2$	−1.6	−1.4	−1.3	−1.6	−1.2	−1.4	
deviation of $C_7-C_2-C_3$	3.4	2.5	2.1	2.8	2.2	2.5	
torsion angle C_7-C_2-X-Z	**52.4**	**52.3**	**51.6**	**51.0**	**42.8**		

[a] Reference 19, the downloaded unit cell was imported to Materials Studio Modeling 3.0 and the values were the "measurements" within the software environment. For the real experimental errors, see the supplementary materials of ref 19. [b] This work, CASTEP, crystal, geometry optimization, gga-pw91, ultrasoft pseudopotential, plane wave cutoff 280 eV. [c] This work, CASTEP, single molecule, geometry optimization, supercell (cubic) sizes: 16 and 20 angstrom, gga-pw91, ultrasoft pseudopotential, plane wave cutoff 280 eV. [d] This work, DMol^3, single molecule, geometry optimization, gga-pw91, all electrons, DNP cutoff 5.5 Å. [e] Reference 41. [f] Reference 42. [g] Reference 33. [h] Z: A point on the S_4 axis, *Z* axis.

from 120° decrease, i.e., a decreasing distortion of the normal, hexagonally symmetric, electronic distribution of benzene. The greatest distortion is in $C(C_6H_5)_4$. Another observation is that the torsion angles of phenyl groups increase as the central bond length X−C increases from tetraphenylmethane to tetraphenyllead. These observations can be explained from the steric hindrance and intramolecular interactions.

The cohesive energy is calculated as the difference between the total energy of the isolated molecule XPh_4 and the total energy of the solid XPh_4 as $E_{coh} = [2E_T(\text{molecular } XPh_4) - E_T(\text{crystlline } XPh_4)]/2$. According to this definition $E_{coh} > 0$ indicates the stable binding state. The calculated E_{coh} energies per molecule (the fourth column of Table 2) at the optimized lattice parameters are consistent with the latent heat of sublimation[52] (listed in the last column of Table 2), except for tetraphenylsilane.

Band Structures, Band Gaps, Density of States (DOS), and Partial Density of States (PDOS). Band structures and density of states (DOS) of solid XPh_4 are shown in Figure 2. To see the band gap, 20 extra empty levels (or virtual orbitals) were added in all the band structure calculations. The valence bands and conduction bands near the Fermi energy were

TABLE 4: Energy Gaps (eV)

	crystal CASTEP minimum band gap	supercell CASTEP, cell 16 Å LUMO−HOMO gap	supercell CASTEP, cell 20 Å LUMO−HOMO gap	isolated molecule DMol^3 LUMO−HOMO gap
CPh_4	4.072	4.258	4.266	4.271
$SiPh_4$	4.230	4.483	4.463	4.497
$GePh_4$	4.282	4.581	4.565	4.585
$SnPh_4$	4.391	4.649	4.678	4.619
$PbPh_4$	4.217	4.611	4.651	4.634

Minimum Band Gap (eV) Estimated from the Band Structure of XPh_4 Crystals

symmetry points in the *k* space	CPh_4	$SiPh_4$	$GePh_4$	$SnPh_4$	$PbPh_4$
Z	4.091	4.230	4.282	4.399	4.272
A	4.184	4.372	4.437	4.503	4.367
M	4.191	4.421	4.523	4.482	4.410
G	4.072	4.341	4.425	4.391	4.217
R	4.156	4.321	4.370	4.457	4.312
minimum band gap (eV)	4.072	4.230	4.282	4.391	4.217

enlarged for detail. The highest valence band edge (∼HOMO) and the lowest conduction band edge (∼LUMO) were indicated by lines with symbols solid triangles and squares, respectively. The conduction bands are comparatively more dispersed than the valence bands because of the relatively strong coupling between nearest neighbor antibonding molecular orbitals. In the plane wave pseudopotential calculations, only electrons on the outer shells (valence electrons) are considered explicitly. The interaction of the valence electrons and the atomic core (consisting of the nucleus and full shell electrons) is represented by a pseudopotential. The valence electrons configurations are as follows: H, $1s^1$; C, $2s^22p^2$; Si, $3s^23p^2$; Ge, $4s^24p^2$; Sn, $5s^2$-$5p^2$; Pb, $6s^26p^25d^{10}$. The total numbers of the valence electrons in a crystal unit cell (2 molecules per cell) are 260 (tetraphenyl lead) and 240 (the rest four crystals). For the ground state, each valence energy level can be filled with 2 electrons (with spin up and down). Therefore the highest occupied electronic state is the 130th (for $PbPh_4$) and 120th (for others) energy level. For crystals from tetraphenylmethane to tetraphenyltin, the 105th to 120th (totally 16) levels are very close and constitute the first valence band. The second valence energy band consists of the 99th to 104th (6) energy levels. Electronic partial density of states (PDOS) analysis (not given here) reveals that the former mainly originates from the p electrons of the carbon atoms on the phenyl rings whereas the latter are from the p electrons of both the central atom (C, Si, Ge, Sn) and the carbon atoms on the phenyl rings. As the atomic number of the central atom increases, the second valence band moves upward and is closer to the first valence band. For tetraphenyl lead, alternatively, the 125th to 130th (6) form the first valence band and the 109th to 124th (16) the second valence band. In this case the two bands essentially blend together. The 121st to 136th (16) energy levels (the 131st to 148th (18) for $PbPh_4$) form the first conduction band; the DOS are primarily contributed from p electrons of carbon atoms on the phenyls and lightly from the p electrons of the central atom of the molecule XPh_4. In addition, the contribution of the central atom to the first conduction band is increased from CPh_4 to $PbPh_4$.

The electronic DOS and PDOS for molecular XPh_4 are illustrated in Figure 3. From these plots one can easily figure out the contributions of constituted atoms of a molecule to the total DOS. The most interesting point is the characteristics of the orbitals near the band gaps. HOMO (H) and LUMO (L) and are shown in Figure 4 and some other frontier orbitals are available in the Supporting Information. The H-7 to H molecular orbitals are composed of π orbital on two or all four phenyl groups. For $SnPh_4$ and $PbPh_4$, some are the combinations of π orbital with the central sp^3-σ orbital. The L to L+7 are of the characters of π^* on phenyl groups or σ^* at the tetrahedral core.

The calculated band gap (for crystals) and LUMO−HOMO gap (for isolated molecules) are summarized in Table 5. For the isolated molecules of XPh_4, the results obtained by the two methods are quite consistent. Employing the supercell approach to molecules, the cell size and the plane wave energy cutoff must be big enough if the results will be comparable to those

TABLE 5: Calculated Refractive Indices in XPh_4 at 650 nm

	X = C				X = Si			
	ref 19		this work		ref 19		this work	
	exptl[a]	calc[b]	calc (SPE)[c]	calc (Geomopt)[d]	exptl[a]	calc[b]	calc (SPE)[c]	calc (Geomopt)[d]
n_e[f] (∥ *c*-axis or *z*-axis)	1.446	1.425	1.867	1.899	1.706	1.755	1.856	1.879
n_o[f] (⊥ *c*-axis or *z*-axis)	1.476	1.455	1.884	1.919	1.742	1.667	1.896	1.926
Δn	0.030	0.030	0.016	0.020	0.036	−0.088	0.041	0.047

	X = Ge				X = Sn			
	ref 19		this work		ref 19		this work	
	exptl[a]	calc[b]	calc (SPE)[c]	calc (Geomopt)[d]	exptl[a]	calc[b]	calc (SPE)[c]	calc (Geomopt)[d]
n_e (∥ *c*-axis or *z*-axis)	1.602	1.649	1.832	1.862	1.757	1.824	1.816	1.830
n_o (⊥ *c*-axis or *z*-axis)	1.647	1.608	1.893	1.917	1.840	1.833	1.888	1.909
Δn	0.045	−0.041	0.061	0.055	0.083	0.009	0.071	0.079

	X = Pb			
	ref 19		this work	
	exptl[a]	calc[b]	calc (SPE)[c]	calc (Geomopt)[d]
n_e (∥ *c*-axis or *z*-axis)	1.730	1.747	1.857	1.891
n_o (⊥ *c*-axis or *z*-axis)	1.789	1.767	1.924	1.965
Δn	0.050	0.020	0.066	0.074

[a] Reference 19, experimental refractive indices in Ph_4X at 650 nm. [b] Reference 19, calculated (using dipole electron shifting model) refractive indices in Ph_4X at 670 nm. [c] This work. Calculated at 650 nm, smearing 0.1 eV, CASTEP single point energy (SPE), at the experimental lattices and geometries. [d] This work. Calculated at 650 nm, smearing 0.1 eV, CASTEP geometry optimization (geomopt), at optimized structures. [e] Reference 52. $n = 1.58 \pm 0.05$, not vary greatly from compound to compound for XPh_4 (X = C, Si, Ge, Sn, Pb) series. [f] n_o and n_e are ordinary and extraordinary refractive indices perpendicular and parallel to the *c*-axis, respectively.

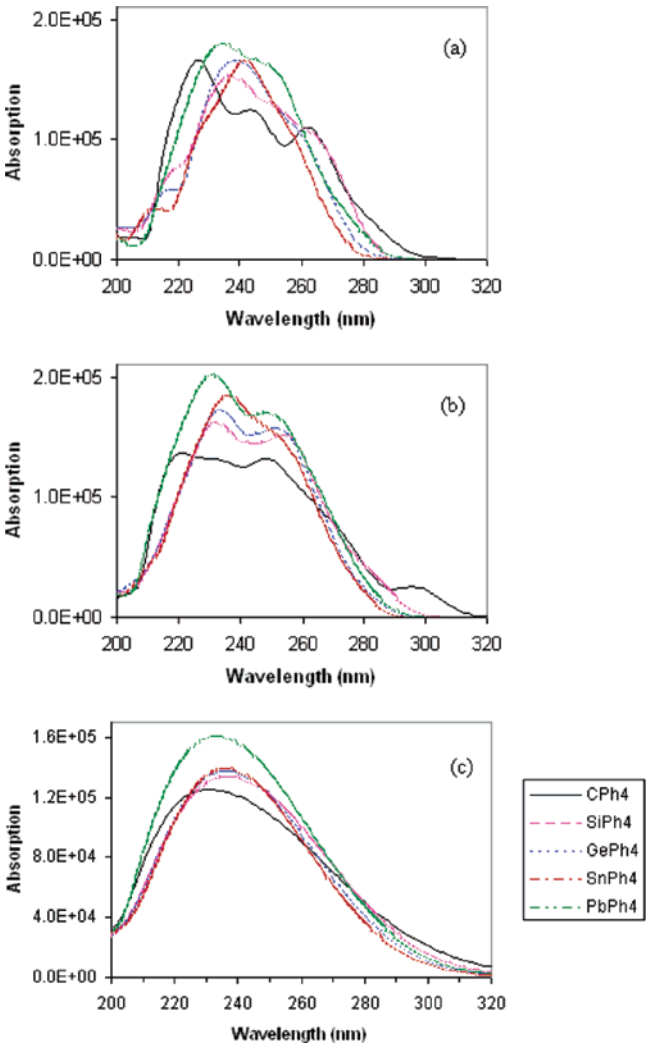

Figure 5. CASTEP optical properties for crystals XPh_4 absorption spectra. (a) Polarized (001) and (b) polarized (100), Gaussian smearing width 0.1 eV. (c) Polycrystalline, Gaussian smearing width 0.3 eV.

calculated by the approach of all electrons calculations with local basis sets. The plane wave pseudopotential method is faster for small and medium molecules. However, as sizes of the tetrahedral molecules increase, the box sizes have to increase proportionally and as a result there is large portion of empty space in the box. As such, one has to pay the penalty (computation cost). Therefore using a local basis sets is appropriate for large molecules.

Optical Properties: Absorption Spectra and Refractive Indices. It is very important to predict and interpret optical (i.e., UV) spectra of materials theoretically and experimentally. Most spectroscopic studies refer to dilute solutions, whereas theoretical works have been focused on the gaseous and solid states. It remains a very challenging task for quantum mechanics methods to investigate the optical properties of especially medium- and large-sized molecules of chemical interest. Furthermore, solute−solvent interactions tune the shape and the intensities of the observed spectra. Thus an inexpensive yet accurate method for calculating vertical excitation energies would be an invaluable tool.

The calculated absorption spectra for crystalline XPh_4 are shown in Figure 5a−c. Spectra in Figure 5a,b were calculated with polarized (001) and (100), respectively, with the Gaussian smearing width of 0.1 eV. Those in Figure 5c were calculated using geometry polycrystalline with smearing of 0.3 eV. The polarizations parallel to and perpendicular to *c*-axis are different. Especially in the curves for CPh_4: three noticeable peaks are observed in Figure 5a that become flat with an additional small peak appearing in Figure 5b. This is possibly caused by the different molecular packings in the crystals, as shown in Figure 1c. The phenyls on adjacent tetraphenyl molecules intercalate along the *a*- or *b*-axis. Along the *c*-axis the packing is layer-by-layer; hence the intermolecular interaction is weak. It has been shown experimentally that materials in this family are essentially transparent from 325 to 1200 nm.[52]

To compare the above calculated results with experimental results, we measured the absorption spectra for the first two members of the family. Tetraphenylmethane (Sigma-Aldrich) and tetraphenylsilane (Pfaltz & Bauer) were recrystallized from chloroform/hexanes before use. The UV spectra were recorded at 20 °C on a UV−vis spectrometer (Shimadzu, UV-2501PC) equipped with a temperature controller (Shimadzu, TCC-240A). Sample concentrations were 1×10^{-5} M (*n*-hexane or THF). The long wavelength absorption maxima for CPh_4 are 272.6 nm (chloroform) and 261.8 nm (*n*-hexane), and for $SiPh_4$ are 264.0 nm (chloroform) and 264.2 nm (*n*-hexane). La Paglia[53,54] has reported the absorption spectra in dilute isooctane solution and emission spectra in the crystalline state at room temperature (excited near the maximum of first transition, i.e., 260 nm) for the group IV tetraphenyls. The author found that the two electronic transitions observed in absorption spectra are analogous to those of benzene and benzene derivatives. Vibrational structures were also analyzed and correlated for all five tetraphenyls.[53] The absorption maxima (in dilute isooctane solution) of the transition 0−0 were 272.5, 271.4, 269.1, and 268.5 nm for XPh_4 (X = C, Si, Ge, Sn), respectively. The calculated refractive indices for the five crystals at 650 nm are presented in Table 5. The crystals are not uniaxial and the difference between the ordinary refractive index (n_o) and the extraordinary refractive index (n_e) increases as the atomic number increases. The refractive indices are 1.83−1.97, in the same range for all five compounds. Our results are something between the following two studies. Newkirk pointed out that the crystals were uniaxially positive with *c*-crystallographic direction containing the optic axis; the refractive indices did not vary greatly from compound to compound and were generally in the range 1.58 ± 0.05 on the basis of the experimental results.[52] Recently, Claborn et al. showed that a strong variation correlated with the polarizability of the central atom by experimental determinations and theoretical calculations using the dipole electron shifting model.[19]

Conclusion

In summary we have investigated the structural and electronic properties of molecules and crystals of tetraphenyl derivatives of group IVA elements. We performed ab initio/DFT calculations to optimize the lattice constants and molecule structures. Band structures, density of states and partial density of states, the energy gaps, and absorption spectra were derived at the optimized structures. Calculated properties were found to be in agreement with experimental data and previously reported ab initio/DFT calculation results. The calculated LUMO−HOMO gaps are 4.1−4.6 eV. The frontier orbitals have significant contributions from the central atoms for $SnPh_4$ and $PbPh_4$. The electronic structures of the XPh_4 molecules calculated with plane wave pseudopotential in supercells are in good agreement with the structures obtained with all electrons and a local basis set DNP.

Supporting Information Available: Tables of geometrical parameters for $GePh_4$, $SnPh_4$, and $PbPh_4$ and a figure showing frontier molecular orbitals. This material is available free of charge via the Internet at http://pubs.acs.org.

References and Notes

(1) Liu, X.-M.; He, C. B.; J.-W. Xu, *Tetrahedron Lett.* **2004**, *45*, 1593.
(2) Chan, L.-H.; Lee, R.-H.; Hsieh, C.-F.; Yeh, H.-C.; Chen, C.-T. *J. Am. Chem. Soc.* **2002**, *124*, 6469.
(3) Chan, L.-H.; Yeh, H.-C.; Chen, C.-T. *Adv. Mater.* **2001**, *13*, 1637.
(4) Yeh, H.-C.; Lee, R.-H.; Chan, L.-H.; Lin, T.-Y. J.; Chen, C.-T.; Balasubramaniam, E.; Tao, Y.-T. *Chem. Mater.* **2001**, *13*, 2788.
(5) Robinson, M. R.; Wang, S.; Heeger, A. J.; Bazan, G. C. *Adv. Funct. Mater.* **2001**, *11*, 413.
(6) Wang, S.; Oldham, W. J., Jr.; Hudack, R. A., Jr.; Bazan, G. C. *J. Am. Chem. Soc.* **2000**, *122*, 5695.
(7) Robinson, M. R.; Wang, S.; Bazan G. C.; Cao, Y. *Adv. Mater.* **2000**, *12*, 1701.
(8) Oldham, W. J., Jr.; Lachicotte, R. J.; Bazan, G. C. *J. Am. Chem. Soc.* **1998**, *120*, 2987.
(9) Laliberte, D.; Maris, T.; Wuest, J. D. *Can. J. Chem.* **2004**, *82*, 386.
(10) Fournier, J.-H.; Wang, X.; Wuest, J. D. *Can. J. Chem.* **2003**, *81*, 376.
(11) Fournier, J.-H.; Maris, T.; Wuest, J. D.; Guo, W.; Galoppini, E. *J. Am. Chem. Soc.* **2003**, *125*, 1002.
(12) Laliberte, D.; Maris, T.; Wuest, J. D. *Acta Crystallogr.* **2003**, *E59*, o799.
(13) Sengupta, S.; Pal, N. *Tetrahedron Lett.* **2002**, *43*, 3517.
(14) Sengupta, S.; Sadhukhan, S. K.; Muhuri, S. *Tetrahedron Lett.* **2002**, *43*, 3521.
(15) Sengupta, S.; Sadhukhan, S. K. *Tetrahedron Lett.* **1999**, *40*, 9157.
(16) Sengupta, S.; Sadhukhan, S. K. *Tetrahedron Lett.* **1998**, *39*, 1237.
(17) Sumsion, H. T.; McLachlan, D. *Acta Crystallogr.* **1950**, *3*, 217.
(18) Robbins, A.; Jeffrey, G. A.; Chesick, J. P.; Donohue, J.; Cotton, F. A.; Frenz, B. A.; Murillo, C. A. *Acta Crystallogr.* **1975**, *B31*, 2395.
(19) Claborn, K.; Kahr, B.; Kaminsky, W. *Cryst. Eng. Commun.* **2002**, *4*, 252.
(20) Zdanov, G. S.; Ismailzade, G. I. *Struct. Rep.* **1949**, *12*, 400.
(21) Zdanov, G. S.; Ismailzade, G. I. *Struct. Rep.* **1950**, *13*, 554.
(22) Glidwell, C.; Sheldrick, G. M. *J. Chem. Soc. A* **1971**, 3127−3129.
(23) Gruhnert, V.; Kirfel, A.; Will, G.; Wallrafen, F.; Recker, K. *Z. Kristallogr.* **1983**, *163*, 53.
(24) Chieh, P. C. *J. Chem. Soc. A* **1971**, 3243−3245.
(25) Karipides, A.; Haller, D. A. *Acta Crystallogr.* **1972**, *B28*, 2889.
(26) Chieh, P. C.; Trotter, J. *J. Chem. Soc. A* **1970**, 911−914.
(27) Akhmed, N. A.; Aleksandrov, G. G *J. Struct. Chem. Engl. Trans.* **1970**, *11*, 824; Ahmed, N. A.; Alexandrov, G. G. *Zh. Struct. Khim.* **1970**, *11*, 891.
(28) Belsky, V. K.; Simonenko, A. A.; Reikhsfeld, V. O.; Saratov, I. E. *J. Organomet. Chem.* **1983**, *244*, 125.
(29) Engelhardt, L. M.; Leung, W.-P.; Raston, C. L.; White, A. H. *Aust. J. Chem.* **1982**, *35*, 2383.
(30) Busetti, V.; Mammi, M.; Signor, A.; Pra, A. D. *Inorg. Chim. Acta* **1967**, *1*, 424.
(31) Preut, H.; Huber, F. *Acta Crystallogr.* **1993**, *C49*, 1372.
(32) Schneider-Koglin, C.; Mathiasch, B.; Draeger, M. *J. Organomet. Chem.* **1994**, *469*, 25.
(33) Csákvári, É.; Shishkov, I. F.; Rozsondai, B.; Hargittai, I. *J. Mol. Struct.* **1990**, *239*, 291.
(34) Ahmed, N. A.; Kitaigorodsky, A. I.; Mirskaya, K. V. *Acta Crystallogr.* **1971**, *B27*, 867
(35) Hutchings, M. G.; Nourse, J. G.; Mislow, K. *Tetrahedron* **1974**, *30*, 1535.
(36) Nourse, J. G.; Mislow, K. *J. Am. Chem. Soc.* **1975**, *97*, 4571.
(37) Hutchings, M. G.; Andose, J. D.; Mislow, K. *J. Am. Chem. Soc.* **1975**, *97*, 4553.
(38) Hutchings, M. G.; Andose, J. D.; Mislow, K. *J. Am. Chem. Soc.* **1975**, *97*, 4562.
(39) Dougherty, D. A.; Mislow, K. *J. Am. Chem. Soc.* **1979**, *101*, 1401.
(40) Charissé, M.; Mathiasch, B.; Dräger, M.; Russo, U. *Polyhedron* **1995**, *14*, 2429.
(41) Knop, O.; Rankin, K. N.; Cameron, T. S.; Boyd, R. J. *Can. J. Chem.* **2002**, *80*, 1351.
(42) Campanelli, A. R.; Ramondo, F.; Domenicano, A.; Hargittai, I. *J. Phys. Chem. A* **2001**, *105*, 5933.
(43) Segall, M. D.; Lindan, P. L. D.; Probert, M. J.; Pickard, C. J.; Hasnip, P. J.; Clark, S. J.; Payne, M. C. *J. Phys.: Condens. Matt.* **2002**, *14*, 2717.
(44) Delley, B. *J. Chem. Phys.* **1990**, *92*, 508.
(45) Delley, *B. J. Chem. Phys.* **2000**, *113*, 7756.
(46) Perdew, J. P.; Wang, Y. *Phys. Rev. B* **1992**, *45*, 13244.
(47) Monkhorst, H.; Pack, J. D. *Phys. Rev. B* **1976**, *13*, 5188.
(48) Francis G. P.; Payne M. C. *J. Phys.: Condens. Matter.* **1990**, *2*, 4395.
(49) Milman V.; Lee M. H.; Payne, M. C. *Phys. Rev. B* **1994**, *49*, 16300.
(50) Fischer, T. H.; Almlof, J. *J. Phys. Chem.* **1992**, *96*, 9768.
(51) Lin, T. T.; He, C. B.; Xiao, Y. *J. Phys. Chem. B* **2003**, *107*, 13788.
(52) Newkirk, H. W. *J. Organomet. Chem.* **1972**, *44*, 263.
(53) La Paglia, S. R. *J. Mol. Spectrosc.* **1961**, *7*, 427.
(54) La Paglia, S. R. *Spectrochim. Acta* **1962**, *18*, 1295.